Available online at www.sciencedirect.com

ScienceDirect

Geochimica et Cosmochimica Acta 160 (2015) 155–168

Geochimica et Cosmochimica Acta

www.elsevier.com/locate/gca

Effects of brine chemistry and polymorphism on clumped isotopes revealed by laboratory precipitation of mono- and multiphase calcium carbonates

Tobias Kluge *,[1], Cédric M. John

Department of Earth Science and Engineering and Qatar Carbonate and Carbon Storage Research Centre, Imperial College London, Prince Consort Road, London, SW7 2BP, UK

Received 7 October 2014; accepted in revised form 29 March 2015; available online 4 April 2015

Abstract

Carbonate clumped isotopes are applied to an increasing number of geological archives to address a wide range of Earth science questions. However, the effect of changes in salinity on the carbonate clumped isotope technique has not been investigated experimentally yet. In particular, evaporated sea water and diagenetic fluids differ substantially from solutions used to calibrate the clumped isotope thermometer as they exhibit high ionic concentrations of e.g., Na^+, Ca^{2+}, Mg^{2+}, and Cl^-. High ionic concentrations are known to have an impact on $\delta^{18}O$ values, and could potentially impact the successful application of clumped isotopes to the reconstruction of diagenetic processes, including precipitation temperatures and the origin of the diagenetic fluid.

In order to address the potential influence of salt ions on the clumped isotope Δ_{47} value we precipitated $CaCO_3$ minerals (calcite, aragonite and vaterite), hydromagnesite and mixtures of these minerals in the laboratory from solutions containing different salt ions (Na^+, Ca^{2+}, Mg^{2+}, Cl^-) at various concentrations and temperatures. The precipitation of some mineralogies was restricted to solutions with specific ionic concentrations, limiting direct comparability. NaCl-rich solutions mostly led to vaterite formation. In control experiments $CaCO_3$ minerals (calcite and aragonite) were precipitated from a $CaCO_3$ supersaturated solution without addition of any other ions.

Our results show that calcium carbonates precipitated from high NaCl concentrations yield Δ_{47} values identical to our NaCl-free control solution. Although addition of Mg led to the formation of hydromagnesite, it also follows the same Δ_{47}-T calibration as calcite. In contrast, Δ_{47} values increase together with increased $CaCl_2$ concentrations, and deviate by a few 0.01‰ from expected equilibrium values.

Overall, clumped isotope values of $CaCO_3$ minerals precipitated between 23 °C and 91 °C (with and without NaCl addition) follow a line with a slope close to results from statistical thermodynamics. We conclude for calcium carbonate and hydromagnesite that the combined effect of salt ion concentration, acid fractionation and polymorphism is negligible for Cl^- and Na^+ with respect to clumped isotope geochemistry, but that offsets are possible in brines containing high concentrations of $CaCl_2$.

1. INTRODUCTION

Carbonates constitute an abundant archive that gives insights into the paleoclimate of different geological epochs, of the geological evolution of sedimentary rocks, and of

* Corresponding author.
E-mail address: tobias.kluge@iup.uni-heidelberg.de (T. Kluge).
[1] Present address: Institut für Umweltphysik, Universität Heidelberg, Im Neuenheimer Feld 229, 69120 Heidelberg, Germany. Tel.: +49 (0)6221 54 6511.

http://dx.doi.org/10.1016/j.gca.2015.03.031
0016-7037/

diagenetic processes in the subsurface (e.g., Miliman, 1974; Tucker and Bathurst, 1990; Moore, 2001; Alonso-Zarza and Tanner, 2010). Bulk carbonate $\delta^{18}O$ and $\delta^{13}C$ values have been successfully used to infer unique paleoclimate information (e.g., Emiliani, 1955; Shackleton and Opdyke, 1976; Zachos et al., 2001), but quantitative interpretations are complicated by the dependence of the carbonate $\delta^{18}O$ value on the parent fluid $\delta^{18}O$ value and the large range of $\delta^{13}C$ values in the dissolved carbon.

These problems can be circumvented by the analysis of multiply-substituted isotopologues in CO_2 produced from acid digestion of carbonates (Eiler, 2007). The abundance of isotopologues of CO_2 containing the rare ^{13}C–^{18}O bonds is governed by temperature-dependent isotope exchange reactions (Wang et al., 2004; Schauble et al., 2006; Cao and Liu, 2012) and is expressed relative to a high temperature stochastic distribution (>1000 °C) denoted as Δ_{47} value (Eiler and Schauble, 2004; Affek and Eiler, 2006). The concomitant occurrence of two rare isotopes in one molecule is described as multiply-substituted isotopologue and often termed 'clumped isotope'. The carbonate clumped isotope proxy is an ideal paleothermometer as the Δ_{47} value is negligibly dependent on the bulk carbonate $\delta^{18}O$ and $\delta^{13}C$ composition (Cao and Liu, 2012) and independent of the parent fluid $\delta^{18}O$ and $\delta^{13}C$ values. The Δ_{47} value under isotopic equilibrium conditions during mineral formation increases with decreasing temperature (~0.004‰ per 1 °C at 50 °C; Wang et al., 2004; Schauble et al., 2006; Ghosh et al., 2006).

Multiply-substituted isotopologues in carbonates (carbonate clumped isotopes) are increasingly used and have already provided significant advances in geothermometry (e.g., Came et al., 2007; Passey et al., 2010; Bristow et al., 2011; Eagle et al., 2011; Halevy et al., 2011). However, possible and so far unexplored effects on the ^{13}C–^{18}O clumping during mineral formation, such as those related to fluid salt ion concentration and mineral structure (polymorphism), are not fully understood. As the popularity of this technique grows and its applications become more diverse, these effects must be constrained to ensure that interpretations based on clumped isotope data account for any fundamental process that occurs during mineral precipitation.

1.1. Potential effects of salt ions on isotope values

Many natural carbonates precipitate in saline fluids, such as marine environments that typically yield salinities of ~35 g/L and mainly contain Na^+ and Cl^- with minor contributions from Mg^{2+}, SO_4^{2-}, Ca^{2+}, and K^+ (Zeebe and Wolf-Gladrow, 2001 and references therein). Mollusks, brachiopods, corals, and foraminifera grow in saline marine waters and are frequently used for paleoclimate reconstruction based on traditional stable isotopes, but also increasingly using clumped isotopes (e.g., Ghosh et al., 2006; Came et al., 2007; Tripati et al., 2010; Csank et al., 2011; Keating-Bitonti et al., 2011; Saenger et al., 2012; Eagle et al., 2013; Grauel et al., 2013; Henkes et al., 2013; Hren et al., 2013).

Other natural fluids beyond sea water often contain a high concentration of Na^+, Mg^{2+}, Ca^{2+} and Cl^- ions. For example, in sedimentary brines and hydrothermal fluids the dissolved salt amount can reach over 300 g/L (e.g., Hanor, 1994; Wilkinson, 2001; Warren, 2006). In particular, Budd et al. (2013) determined salinities of up to 17.8 wt% NaCl (~220 g/L) in diagenetic fluids from fluid inclusion analysis. Newell and Goldstein (1999) and Rossi et al. (2002) observed salinities of up to 24 wt% NaCl (~315 g/L) in fluid inclusions of quartz crystals. Accordingly, diagenetic processes often involve highly saline fluids that are significantly different from solutions used to experimentally calibrate the carbonate clumped isotope thermometer. There are various experimental calibrations (Ghosh et al., 2006; Dennis and Schrag, 2010; Zaarur et al., 2013; Fernandez et al., 2014; Tang et al., 2014; Defliese et al., 2015), none of which have used parent fluids that reflect the full range of salinities of natural fluids. Ghosh et al. (2006) established the first clumped isotope calibration, where calcite was precipitated from a solution containing only Ca^{2+}, HCO_3^- and CO_3^{2-} ions at temperatures ranging between 1 and 50 °C. Zaarur et al. (2013) used the same approach to refine the commonly cited calibration of Ghosh et al. (2006).

Given that there is a common mechanism for clumped and oxygen isotopes, salinity may also influence the Δ_{47}-T relationship. Evidence for ionic effects are known from oxygen isotopes where studies found a significant effect of ionic concentrations on the liquid–vapour fractionation (Taube, 1954; Sofer and Gat, 1972; O'Neil and Truesdell, 1991; Driesner and Seward, 2000; Kim et al., 2012). Measurements of CO_2 equilibrated with a solution containing various ions revealed a dependence of the $\delta^{18}O$ value in CO_2 on the salt concentration and the dominating salt ion (Taube, 1954; O'Neil and Truesdell, 1991). The greatest effects of up to several per mil (‰) were observed for ions that exhibit the strongest covalent character of the ion–water interaction (e.g., Al^{3+}, Mg^{2+}). In contrast, ions that possess a similar strength of the ion–water interaction compared to water–water interaction (e.g., Na^+) have a negligible effect on the $\delta^{18}O$ value of CO_2 in equilibrium with the solution. These effects can be explained by the number of water molecules that get 'bound' to a certain ion (i.e. the apparent hydration number) and that are therefore no longer freely available for isotopic exchange with CO_2 (e.g., Frank and Wen, 1957). The potential to attach water molecules to the ion separates the water into at least two distinct groups: water bound to the solutes in the hydration sphere and free unhydrated water that behaves similar to pure water (Taube, 1954). This separation can influence the isotopic composition of the free water and the isotope exchange reactions between the relatively free water molecules in the unhydrated water (relative to the bound water) and dissolved inorganic carbon (DIC). Structure-making electrolytes (e.g., $MgCl_2$, $CaCl_2$) lead to the concentration of ^{18}O in the hydration sphere, whereas structure-breaking electrolytes (KCl, CsCl) prefer ^{16}O in the hydration sphere (e.g. O'Neil and Truesdell, 1991).

It is uncertain what effect different ions in a solution have on the ^{13}C–^{18}O clumping of the DIC. The ^{13}C–^{18}O clumping is mainly determined by the characteristics of the involved C–O bond (e.g., bond order; Schauble et al.,

2006), which can lead to variations in the isotope exchange reactions. The abundance of ^{13}C–^{18}O bonds in the DIC species should be unaffected by ionic effects after isotopic equilibrium between bound and free water was reached. Most carbonate and bicarbonate ions interact with the dominating free water (a minor fraction with the generally much smaller bound component). As the Δ_{47} value does not depend on the solution isotope values (Cao and Liu, 2012), carbonate and bicarbonate ions should yield the equilibrium clumped isotope value once isotope exchange equilibrium in bound and free water is established. Under kinetic conditions, e.g., during fast mineral growth where attached water molecules are rapidly stripped off the hydration spheres, the relative rate of isotope exchange between free and hydrated water as well as between free water and (bi)carbonate ions becomes important and discrimination may occur between ^{12}C–^{16}O–^{16}O–^{16}O and ^{13}C–^{18}O–^{16}O–^{16}O.

1.2. Potential effects of polymorphism on isotope values

The mineralogy of carbonates could potentially affect the Δ_{47} value in two ways; firstly by the effect on the equilibrium constant for the isotope exchange reaction relevant to ^{13}C–^{18}O bonds during mineral precipitation, and secondly, by the mineral-dependent acid fractionation during phosphoric acid digestion. Although theoretical calculations of the ^{13}C–^{18}O clumping during carbonate mineral formation show only a small effect of the crystal structure on the equilibrium constant (Schauble et al., 2006), increased ^{13}C–^{18}O clumping is expected in Mg-bearing minerals and in orthorhombic carbonates (e.g., aragonite; Schauble et al., 2006). According to calculations based on density functional perturbation theory this could result in an equilibrium constant 0.02‰ higher for aragonite and 0.01‰ higher for magnesite at 25 °C (Schauble et al., 2006). Additionally, isotopic fractionation occurs during phosphoric acid digestion of the carbonate mineral, altering the Δ_{47} value. Cluster models suggest that the phosphoric acid fractionation of Δ_{47} for aragonite and calcite is similar, whereas for magnesite it is 0.03‰ lower (Guo et al., 2009). Combined with the ^{13}C–^{18}O clumping related to the mineral formation (Schauble et al., 2006) aragonite Δ_{47} values are expected to be higher by ~0.02‰ compared to calcite at any given Earth surface temperature. In contrast, magnesite and dolomite Δ_{47} values are expected to be lower by ~0.02‰. These effects seem to be small, but if not accounted for would contribute to a temperature error of ~6 °C at low temperatures (~25 °C), ~12 °C at 100 °C, or 25 °C at 200 °C (using the calcite Δ_{47}-T calibration of Kluge et al., 2015). These temperature differences are substantial and would have a significant impact on interpretations of paleoenvironments and diagenetic histories. Despite a large number of studies of different biogenic $CaCO_3$ polymorphs (e.g., calcitic and aragonitic mollusks and brachiopods; Came et al., 2007, 2014; Eagle et al., 2013; Henkes et al., 2013), it still remains to be experimentally confirmed whether there is a mineral-related effect on the ^{13}C–^{18}O clumping, and if the model calculations accurately reproduce the effect of $CaCO_3$ polymorphism.

In this study we aim to experimentally determine (a) what influence the salt ion effect has on ^{13}C–^{18}O clumping, and (b) whether mineralogy affects the Δ_{47} value inherited from the solution. We precipitated a suite of carbonates under controlled conditions (temperature, ion concentration) in the laboratory to address these aims. About half of the experiments resulted in pure $CaCO_3$ phases, whereas the rest consists of a mixture of $CaCO_3$ polymorphs. The fact that the samples are composed of multiple $CaCO_3$ phases complicates the independent assessment of salt ion effect and mineralogy, but still allows quantification of the combined effect.

2. METHODS

2.1. Laboratory precipitation of carbonate minerals and sample screening

The experiments were conducted in an analogous fashion to the experiments of McCrea (1950), O'Neil et al. (1969), and Kim and O'Neil (1997). As the initial calibration of the carbonate clumped isotope thermometer (Ghosh et al., 2006) and the recent refinement (Zaarur et al., 2013) used the same method, it allows direct comparison with our experimental results. We used two different growth solutions, one with a low ionic concentration that only consisted of a solution with reverse osmosis water (processed with an Ultrapure™ 18 MΩ system) and dissolved calcite (0.007 molal Ca^{2+}; similar to the clumped isotope temperature calibration of Ghosh et al., 2006) and one with added NaCl, $CaCl_2$ or $MgCl_2(H_20)_6$ (up to 6.5 molal for NaCl, 1.8 molal for $CaCl_2$, and 0.7 molal for $MgCl_2(H_2O)_6$; Table 1). Temperatures for individual experiments were adjusted to fixed values between 23 and 91 °C. The solutions were prepared by dissolving ~360 mg of high-purity calcite (Merck Suprapur, 99.95% calcium carbonate) into 500 mL deionized water. Continuous CO_2 bubbling through the stirred solution led to dissolution of the added calcite. The solution was filtered after 2–3 h of CO_2 bubbling to remove any undissolved calcite. Subsequently, the DIC in the solution was isotopically equilibrated with water at the intended experiment temperature for a minimum of 2 h (91 °C) up to 24 h (25 °C, time scales based on Beck et al., 2005) before salts were added (optional, for the experiments Mg-1 to Mg-3 and CA-1 to CA-3 salt was added prior to isotopic equilibration). Equilibration times for water-DIC exchange are oriented at the values for oxygen isotopes as the experiments of Affek (2013) showed that the equilibration time scales for CO_2 clumped isotopes are comparable to that of oxygen isotopes. For equilibration the solution inside the Erlenmeyer flask was stored in the water bath. At a water bath temperature above 50 °C a constant and low CO_2 flow through the solution was maintained during the equilibration phase to avoid precipitation of carbonates. In order to induce carbonate precipitation the equilibrated solution was slowly purged with nitrogen for up to several days (bubbling rate of ~1 bubble per second). The pH was monitored in several experiments to assess the evolution of the solution (Fig. 1). At the beginning of the slow N_2 bubbling

Table 1
Experimental conditions during laboratory carbonate precipitation following the methods of McCrea (1950) and O'Neil et al. (1969), and X-ray diffraction results. The uncertainty in the mineral phase quantification is about 3%.

Experiment No.	$CaCO_{3,dissolved}$ (g/l)	T (°C)	Added salts (g/l)	Equilibration (h)	Precipitation (h)	Mineralogy
No salt added						
1	0.74	23.5 ± 0.5	–	17	147	Calcite
2	1.00	25.7 ± 0.5	–	15	72	Calcite
3	0.70	37.5 ± 0.5	–	17	100	Calcite
4	0.60	49.6 ± 0.5	–	15	30	Calcite (55%), aragonite (45%)
5	0.74	49.6 ± 0.5	–	17	195	Calcite
6	0.60	69.9 ± 0.5	–	17	44	Calcite (57%) aragonite (43%)
7	0.76	69.9 ± 0.5	–	18	25	Calcite (90%) aragonite (10%)
8	0.70	79.9 ± 0.5	–	3	~20	Calcite (78%) aragonite (22%)
9	0.78	91.0 ± 0.5	–	2	22	Calcite (72%) aragonite (28%)
10	0.74	91.0 ± 0.5	–	3	138	Aragonite (83%), calcite (17%)
NaCl added						
NA-1	0.68	23.5 ± 0.5	250	23	451	Vaterite
NA-2	0.60	25.7 ± 0.5	300	15	168	Calcite, aragonite*
NA-3	0.70	37.5 ± 0.5	260	21	72	Vaterite (95%), calcite (5%)
NA-4	0.74	37.5 ± 0.5	244	14	341	Vaterite (>95%), rest: calcite
NA-5	0.70	49.6 ± 0.5	375	16	143	Vaterite
NA-6	0.80	49.6 ± 0.5	262	17	573	Vaterite
NA-7	0.70	69.9 ± 0.5	325	3	69	Vaterite
NA-8	0.78	79.9 ± 0.5	280	3	47	Calcite (49%), aragonite (24%), vaterite (27%)
NA-9	0.70	91.0 ± 0.5	260	3	42	Vaterite (94%), aragonite (6%), calcite (<1%)
$CaCl_2$ added						
CA-1	0.74	79.9 ± 0.5	26	3	164	Calcite
CA-2	0.70	79.9 ± 0.5	48	3	164	Calcite
CA-3	0.74	79.9 ± 0.5	98	15	192	Calcite
CA-4	0.77	25.7 ± 0.5	100	24	312	Calcite*
CA-5	0.72	25.7 ± 0.5	200	25	502	Calcite*
$MgCl_2(H_2O)_6$						
Mg-1	0.66	79.9 ± 0.5	50	15	142	Hydromagnesite (88%), aragonite (12%)
Mg-2	0.70	79.9 ± 0.5	102	16	241	Brucite
Mg-3	0.86	79.9 ± 0.5	150	14	315	Hydromagnesite

* Checked via light microscopy only.

the pH value increased typically to ~7.5, where the main fraction of the minerals formed. Generally no mineral growth was observed during the first 24 h when the main pH change of the solution occurred. As the time required for 99% DIC-water equilibration at 25 °C is below 2 h at pH < 7.5 (following Uchikawa and Zeebe, 2012) no disequilibrium effects are expected from the initial pH changes. Furthermore, for pH 7.7–9 HCO_3^- is the dominating DIC species (>95%) for pure water with a fraction that only marginally changes with pH in this range. Isotopic disequilibrium effects related to changes in the DIC speciation are therefore unlikely for low-salinity water. In case of significant salt addition the DIC composition changes towards CO_3^{2-} and an increase in the equilibration time is expected (Uchikawa and Zeebe, 2012). Although relevant for all experiments with NaCl addition and experiments Mg-3, Ca-3 to Ca-5, we prevented an incomplete isotope exchange by equilibrating the solution with the DIC at the experiment temperature prior to salt addition (except Mg-3 and Ca-3, where salts were added prior to equilibration).

The precipitated calcite crystals were filtered from the solution and inspected microscopically and via X-ray diffraction before analysing them for clumped isotopes. The precipitation experiments were repeated if not enough carbonate was formed for three or more Δ_{47} measurements per precipitation temperature (Table 2).

XRD measurements were performed at the National History Museum London using an Enraf Nonius FR 590 Powder Diffractometer with Cu Kα radiation that was operated at 40 kV and 35 mA. Carbonate samples were placed as a thin layer on a sapphire substrate and were measured in a fixed beam-sample-detector geometry with a 5° incidence angle between X-ray beam and sample using an INEL 120° position-sensitive detector. Analysis times varied between 10 and 90 min depending on counting statistics and step size. The signals were evaluated by a computer-routine (X'Pert Highscore, PANalytical B.V., 2009) that compares measured spectra with a mineral data base. Peak positions were calibrated with two standards (silver behenate; Blanton et al., 1995; and quartz). Pure calcite

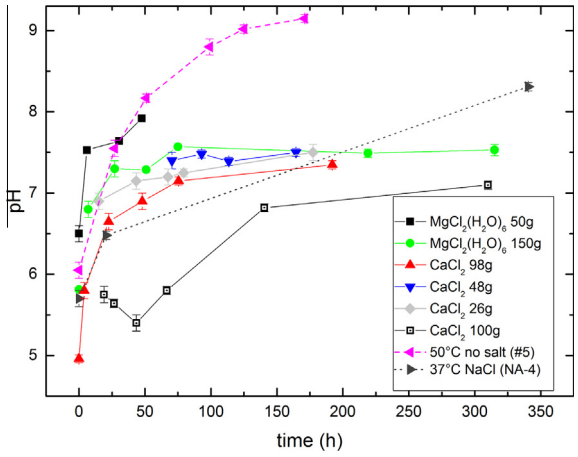

Fig. 1. pH evolution during carbonate precipitation. Precipitated carbonate was typically observed after approximately one day, with the exception of the $CaCl_2$ where carbonate was typically observed after a few hours. In the case of Ca-5 ($CaCl_2$ 100 g) significant precipitation started only after 6 days. Mg and NaCl addition delayed the initiation of carbonate precipitation by up to several days. The initial increase in the pH values is due to the slow CO_2 degassing by controlled N_2 bubbling.

and aragonite standards were measured for phase quantification. The aragonite and calcite phase fraction was determined via comparison with the pure standards using an automated routine of the X'Pert Highscore software and/or manual evaluation using peak intensities.

2.2. Sample treatment for carbonate clumped isotope analysis

Individual samples consisting each of 5–8 mg carbonate were inserted into the inlet part of a reaction vessel that allows sample storage separate from the 105% phosphoric acid at the bottom (1.5–3 ml per sample). Each sample aliquot was reacted separately in a cleaned reaction vessel with new acid (Supplementary Fig. S1). No common acid bath was used. The reaction vessel, containing carbonate sample and ortho-phosphoric acid, was evacuated for 30 min and typically reached pressures of 10^{-1}–10^{-2} mbar before the acid digestion was started. At 90 °C $CaCO_3$ was reacted with ortho-phosphoric acid for 10 min in the stirred reaction vessel and the evolving CO_2 continuously trapped. At the beginning of the study $CaCO_3$ samples were reacted at 70 °C for 15 min (Table 2) according to the laboratory practice at this time, before the procedure was changed to 90 °C for all experiments. The reaction times at 70 °C and 90 °C extended beyond the point when bubble formation in the acid ceased and thereby ensured a complete phosphoric acid reaction. The reactant CO_2 was cleaned using a procedure analogous to that of Dennis and Schrag (2010). In brief, the evolved CO_2 was continuously trapped during the phosphoric acid reaction in a liquid-N_2-cooled trap. Subsequently, potential atmospheric components were cryogenically separated from the liquid-N_2-cooled trap. Water was then separated from CO_2 in this trap using a dry-ice ethanol mixture. The CO_2 gas was afterwards passively passed through a glass trap filled with silver wool and another trap densely packed with Porapak Q (filled length: 13 cm, inner diameter: ~8 mm) held at −35 °C. The purified CO_2 gas was transferred to the mass spectrometer for analysis. A schematic diagram of the procedure is shown in the Supplementary (Fig. S2).

2.3. Mass spectrometric analysis and data evaluation

Mass spectrometric analyses were performed on two isotope ratio mass spectrometers (MAT 253, Thermo Scientific) in the Qatar Stable Isotope Lab at Imperial College. The analysis followed the procedures described by Huntington et al. (2009) and Dennis et al. (2011). A measurement consisted of 8 cycles with 7 sequences per cycle and an integration time of 26 s per sequence (in total ~1460 s for sample and reference gas, respectively). Each cycle included a peak center, background measurements and an automatic bellows pressure adjustment aimed at a 15V signal at mass 44. The sample gas was measured against an Oztech reference standard ($\delta^{13}C = -3.63‰$ VPDB, $\delta^{18}O = -15.79‰$ VPDB and $\delta^{13}C = -3.62‰$ VPDB, $\delta^{18}O = -15.73‰$ VPDB, respectively). Heated gases (1000 °C), water-equilibrated gases (25 °C, 50 °C, 80 °C), a Carrara Marble carbonate standard and a carbonate standard provided by ETH Zurich (data in Supplementary) were measured regularly to transfer the raw Δ_{47} values into the CO_2 equilibrium scale reference frame ('CDES'; Dennis et al., 2011). Potential sample contamination was monitored using the mass 48 and mass 49 signals (Eiler and Schauble, 2004; Huntington et al., 2009). Sample measurements were rejected based on elevated 48 and 49 signals following the procedures of Huntington et al. (2011). Threshold values were considered to be deviations of sample mass-48 of more than 2‰ from that of clean standards and a mass-49 parameter >0.2 (mass-49 parameter = (sample 49 signal (mV)/sample 44 signal (mV) − standard 49 signal (mV)/standard 44 signal (mV)) * 1000). Replicate measurements were spread out over several months to exclude effects of potential short-term variability of mass spectrometer signals.

Raw Δ_{47} values were first linearity-corrected using the heated gas data (Huntington et al., 2009) and then transferred into the CO_2 equilibrium scale of Dennis et al. (2011) using empirical transfer functions (ETF). Primary ETFs were established based on equilibrated and heated gases and were additionally used to determine the phosphoric-acid-correction-free Δ_{47} values of carbonate standards in the CDES. Once Δ_{47} values of carbonate standards were established, a secondary transfer function was established based on heated gases and gas evolved from carbonates (ETFs and standard values are given in the Supplementary). Secondary ETFs have to be determined if no equilibrated gases were measured and the transfer into the CDES is mainly based on carbonate standards (Dennis et al., 2011). Average Δ_{47} values for Carrara marble in the CDES were $0.389 \pm 0.003‰$ (1 SE, $n = 74$, machine 1) and $0.386 \pm 0.006‰$ (1 SE, $n = 23$, machine 2) in agreement with published values (Dennis et al., 2011). A phosphoric acid correction was applied to carbonate samples after the Δ_{47} values were transferred into the CDES. For acid

Table 2
Δ_{47}, $\delta^{18}O$, and $\delta^{13}C$ values of laboratory carbonate precipitates. $\delta^{18}O_{water}$ is the calculated solution isotope value based on the carbonate $\delta^{18}O$ value and the mineral-specific fractionation factor (see Section 2.3). *n* indicates the number of replicates measured. The uncertainties are given as standard error for the Δ_{47} values and as 1σ standard deviation for $\delta^{18}O$ and $\delta^{13}C$. Samples marked by '+' were reacted at 90 °C, '*' indicates that part of the replicates were reacted at 90 °C. All other samples were digested with phosphoric acid at 70 °C.

Experiment no.	*T* (°C)	Δ_{47} (‰)	$\delta^{18}O$ (‰)	$\delta^{13}C$ (‰)	$\delta^{18}O_{water}$ (‰)	*n* (−)
No salt added						
1	23.5 ± 0.5	0.691 ± 0.004	−8.24 ± 0.08	−18.51 ± 0.04	−6.4 ± 0.1	3
2	25.7 ± 0.5	0.706 ± 0.010	−8.40 ± 0.51	−17.05 ± 0.11	−6.1 ± 0.5	3
3*	37.5 ± 0.5	0.670 ± 0.023	−12.38 ± 0.18	−20.61 ± 0.11	−7.8 ± 0.2	4
4	49.6 ± 0.5	0.625 ± 0.016	−13.51 ± 0.28	−19.04 ± 0.01	−6.8 ± 0.3	2
5+	49.6 ± 0.5	0.628 ± 0.013	−14.04 ± 0.11	−28.23 ± 0.10	−7.4 ± 0.1	3
6	69.9 ± 0.5	0.584 ± 0.020	−15.43 ± 0.01	−19.42 ± 0.01	−5.6 ± 0.1	2
7	69.9 ± 0.5	0.577 ± 0.008	−16.89 ± 0.11	−23.22 ± 0.12	−7.0 ± 0.2	3
8*	79.9 ± 0.5	0.562 ± 0.012	−17.07 ± 0.37	−25.07 ± 0.21	−5.7 ± 0.4	8
9	91.0 ± 0.5	0.528 ± 0.007	−18.84 ± 0.10	−24.34 ± 0.07	−6.0 ± 0.1	3
10+	91.0 ± 0.5	0.521 ± 0.026	−20.60 ± 0.08	−31.20 ± 0.01	−8.1 ± 0.1	2
NaCl added						
NA-1	23.5 ± 0.5	0.689 ± 0.003	−8.57 ± 0.16	−18.21 ± 0.06	−6.8 ± 0.2	3
NA-2	25.7 ± 0.5	0.698 ± 0.008	−8.70 ± 0.16	−18.50 ± 0.07	−6.4 ± 0.2	3
NA-3	37.5 ± 0.5	0.639 ± 0.020	−11.29 ± 0.20	−20.39 ± 0.10	−6.8 ± 0.1	1
NA-4+	37.5 ± 0.5	0.672 ± 0.027	−13.30 ± 0.37	−26.06 ± 0.18	−8.8 ± 0.4	3
NA-5	49.6 ± 0.5	0.605 ± 0.005	−13.85 ± 0.26	−21.39 ± 0.03	−7.2 ± 0.3	2
NA-6+	49.6 ± 0.5	0.634 ± 0.008	−15.06 ± 0.22	−25.26 ± 0.17	−8.4 ± 0.2	3
NA-7	69.9 ± 0.5	0.577 ± 0.010	−16.92 ± 0.15	−21.71 ± 0.03	−7.0 ± 0.2	3
NA-8	79.9 ± 0.5	0.553 ± 0.018	−17.54 ± 0.03	−25.86 ± 0.10	−6.3 ± 0.1	3
NA-9*	91.0 ± 0.5	0.545 ± 0.005	−19.21 ± 0.15	−25.00 ± 0.16	−6.3 ± 0.2	5
$CaCl_2$ added						
CA-1+	79.9 ± 0.5	0.558 ± 0.010	−18.21 ± 0.18	−30.22 ± 0.08	−6.8 ± 0.2	3
CA-2+	79.9 ± 0.5	0.548 ± 0.017	−17.65 ± 0.06	−30.37 ± 0.05	−6.2 ± 0.1	3
CA-3+	79.9 ± 0.5	0.588 ± 0.014	−16.95 ± 0.26	−28.85 ± 0.02	−5.5 ± 0.3	3
CA-4+	25.7 ± 0.5	0.713 ± 0.016	−8.70 ± 0.26	−23.05 ± 0.15	−6.4 ± 0.3	4
CA-5+	25.7 ± 0.5	0.750 ± 0.003	−10.00 ± 0.08	−26.35 ± 0.18	−7.7 ± 0.1	2
$MgCl_2(H_2O)_6$						
Mg-1+	79.9 ± 0.5	0.568 ± 0.006	−16.96 ± 0.27	−17.70 ± 0.06	−9.0 ± 0.3	3
Mg-2+	79.9 ± 0.5	0.577 ± 0.020	−12.81 ± 0.20	−5.74 ± 0.10	–	1
Mg-3+	79.9 ± 0.5	0.571 ± 0.011	−16.14 ± 0.10	−16.76 ± 0.01	−8.6 ± 0.1	4

digestion of calcite we used a correction of 0.069‰ at 90 °C and of 0.052‰ at 70 °C (based on Guo et al., 2009; Eq. 23 therein), and applied the same fractionation factor to all measured carbonates. This approach is justified for the $CaCO_3$ polymorphs calcite and aragonite as, for example, the study of Wacker et al. (2013) and Defliese et al. (2015) did not find a significant difference between the acid fractionation factors of aragonite and calcite. Note that the acid digestion correction of Guo et al. (2009) is a theoretical estimate based on ab-intio calculation and transition state theory. Experimental studies that reacted samples at 90 °C derived acid fractionation factors ranging from ~0.07 to ~0.09‰ (Passey et al., 2010; Henkes et al., 2013; Wacker et al., 2013; Defliese et al., 2015).

Carbonate $\delta^{18}O$ values were calculated using the acid fractionation factors of Kim and O'Neil (1997) with the correction of Böhm et al. (2000) for calcite, the acid fractionation factors of Kim et al. (2007b) for aragonite, and of Das Sharma et al. (2002) for hydromagnesite (assumed to be similar to magnesite). Mixtures of calcite (or hydromagnesite) and aragonite crystals were evaluated using the corresponding fractionation factors and the ratio of calcite (or hydromagnesite) to aragonite. For vaterite the calcite fractionation factor was used due to the lack of studies that explicitly investigated the oxygen isotope fractionation factor between vaterite and water. The studies of Tarutani et al. (1969) and Kim and O'Neil (1997) suggest an enrichment of vaterite relative to calcite of 0.5 and 0.6‰, respectively.

Water $\delta^{18}O$ values were not directly determined on the solution, but back-calculated from the carbonate $\delta^{18}O$ using the water-carbonate fractionation factors of Kim and O'Neil (1997) for calcite, of Kim et al. (2007a) for aragonite, and of O'Neil and Barnes (1971) and Friedman and O'Neil (1977) using the equation of Zedef et al. (2000) for hydromagnesite. Mixtures were proportionally evaluated using the corresponding fractionation factors.

The analytical uncertainties of Δ_{47}, $\delta^{18}O$ and $\delta^{13}C$ measurements were calculated by Gaussian error propagation. We used the standard error (SE) of the mean in the case of replicate analyses and the standard deviation for a single measurement (1σ: ~0.02‰ for Δ_{47}, 0.2‰ for $\delta^{18}O$, and 0.1‰ for $\delta^{13}C$). The typical standard deviation of a single measurement was deduced from the long-term analysis of

carbonate standards and agrees with the reproducibility of samples.

3. RESULTS

XRD analyses confirmed all minerals to be polymorphs of $CaCO_3$, with the exception of experiments involving Mg where hydromagnesite and brucite was precipitated (Table 1). At lower temperatures calcite was prevalent in experiments without salt addition, whereas the precipitates at higher temperatures ($\geqslant 50$ °C) consisted of a mixture of calcite and aragonite (Table 1). No pure aragonite precipitate was observed. NaCl addition led to the formation of vaterite (Kluge and John, 2014). Increased levels of $CaCl_2$ favoured the precipitation of pure calcite. The addition of Mg led to the precipitation of a hydromagnesite/aragonite mixture at low Mg concentrations (0.25 molal $MgCl_2(H_2O)_6$) and exclusively to hydromagnesite at higher concentrations.

The $\delta^{18}O$ value of the solution was calculated from the carbonate $\delta^{18}O$ value using the experimental temperature and the fractionation factors corresponding to the precipitated mineral (see Section 2.3). The solution $\delta^{18}O$ value was calculated to check for potential kinetic effects that could occur during mineral precipitation. The laboratory reverse osmosis water was processed from local tap water that has an isotopic composition similar to ground and surface water in the London Metropolitan area (−6‰ to −8‰, Darling et al., 2003). The calculated solution water $\delta^{18}O$ values yield an average of -6.5 ± 0.6‰ in 2012 and of -8.4 ± 0.6‰ in 2013 (Supplementary Fig. S3). No systematic trends are observed in relation to the experiment temperature (Supplementary Fig. S4), generally suggesting neither a kinetic effect during mineral formation nor evaporative change of the solution $\delta^{18}O$. Exceptions are the experiments where $CaCl_2$ was added. In these cases the back-calculated water $\delta^{18}O$ values are elevated at higher $CaCl_2$ concentrations (Table 1).

The Δ_{47} values of replicate measurements of the laboratory precipitates vary between 0.750 ± 0.003‰ (1 SE) and 0.521 ± 0.026‰ (1 SE) corresponding to the experimental temperature range of 23 °C to 91 °C (Table 2). Addition of NaCl resulted in no statistical significant deviation from NaCl-free $CaCO_3$ minerals (Table 2, Fig. 2). Comparing samples measured on the same day and on the same mass spectrometer, the maximum difference in Δ_{47} of samples precipitated from the NaCl brine relative to samples from a NaCl-free solution was observed for carbonates precipitated at 70 °C, but their Δ_{47} values agree within the 1σ-standard deviation. On average, the difference between $CaCO_3$ minerals formed from a solution with and without NaCl is -0.003 ± 0.008‰ (1σ), considering only samples measured on the same day, and -0.001 ± 0.010‰ (1σ) taking into account all measurements. This result suggests that a potential salt ion effect on ^{13}C–^{18}O clumping is below the limit of current instrumental precision or, alternatively, that the effects of NaCl, acid fractionation and $CaCO_3$ polymorphism are each small and compensate each other.

Addition of varying amounts of $CaCl_2$ (0.24–1.80 molal) led to the formation of calcite minerals yielding Δ_{47} values

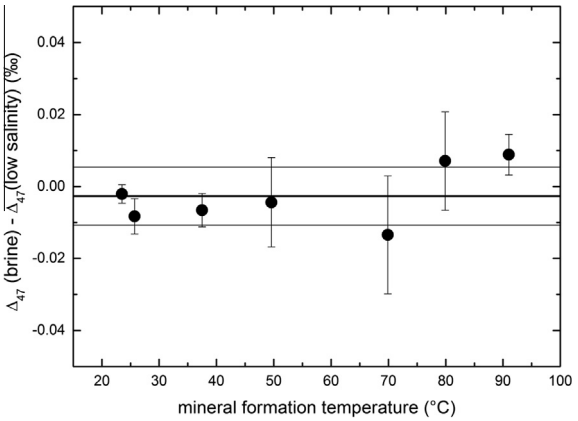

Fig. 2. Differences in the Δ_{47} values of $CaCO_3$ minerals precipitated with and without NaCl addition (brine and low-salinity solution, respectively). Carbonates precipitated under both conditions were measured either at the same day or within a few days of each other to minimize potential session-specific analytical bias. The thick black line and the two thin lines represent the mean Δ_{47} difference and its 1σ standard deviation (-0.003 ± 0.008‰).

that deviate from the reference solution in particular at elevated $CaCl_2$ concentration (Table 2, Fig. 3). At a growth temperature of 80 °C the highest offset of 0.029 ± 0.017‰ was observed at the highest $CaCl_2$ concentration (0.89 molal). A repeat experiment at 25 °C with $CaCl_2$ concentrations of ~0.9 and 1.8 molal led to similar offsets of 0.011 ± 0.021‰ and 0.048 ± 0.013‰, respectively. These offsets were calculated using the combined average Δ_{47} value of all experiments at 80 °C with and without NaCl as salt-free reference.

$MgCl_2(H_2O)_6$ addition resulted in the precipitation of hydromagnesite and brucite. Hydromagnesite shows no significant offset (0.010 ± 0.015‰). Therefore, Δ_{47} values of

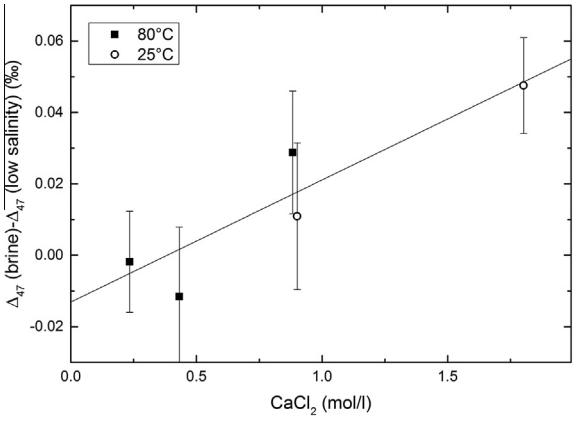

Fig. 3. Differences in the Δ_{47} values of carbonate minerals precipitated with and without $CaCl_2$ addition (brine and low-salinity solution, respectively). The values were calculated by comparing the sample carbonate Δ_{47} values with the average Δ_{47} value of $CaCO_3$ precipitated from a $CaCl_2$-free solution at the same temperature (80 °C and 25 °C, respectively; includes the NaCl-brine data). The solid line is a linear regression of the Δ_{47} difference against the solution $CaCl_2$ concentration ($R^2 = 0.72$).

hdyromagnesite seem to be indistinguishable from $CaCO_3$ minerals precipitated from Mg-free solutions if the same acid fractionation factor is used (Table 2, Fig. 4). In one experiment only a minor, unidentifiable carbonate fraction precipitated together with brucite and is therefore not discussed further.

Average Δ_{47} values of all samples (with and without added NaCl) at a given temperature follow a Δ_{47}-T slope of $4.00 \pm 0.18 \cdot 10^4/T^2$ (T in K; $R^2 = 0.97$). This value overlaps with an error-weighted fit of carbonates from the NaCl-free solution ($4.14 \pm 0.23 \cdot 10^4/T^2$, $R^2 = 0.96$) and with that of a linear regression based on theoretical calculations for the investigated temperature interval ($3.95 \cdot 10^4/T^2$, Fig. 5; linear approximation over $1/T^2$ from 0 to 100 °C of Schauble et al., 2006 and Guo et al., 2009). Furthermore, the Δ_{47}-T slope agrees with recent synthetic calibration studies that acid-reacted carbonates at elevated temperatures of 90 °C or 100 °C (Dennis and Schrag, 2010; Passey and Henkes, 2012; Fernandez et al., 2014; Tang et al., 2014) and is discussed in Kluge et al. (2015).

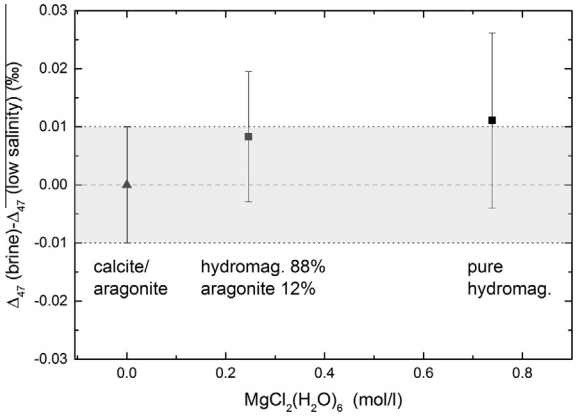

Fig. 4. Differences in the Δ_{47} values of carbonate minerals precipitated with and without $MgCl_2(H_2O)_6$ addition. The values are calculated by comparing the sample carbonate Δ_{47} values with the Δ_{47} value of $CaCO_3$ precipitated from a Mg-free solution at the same temperature (80 °C). The grey shaded area indicates the 1 SE uncertainty of the Mg-free carbonate reference.

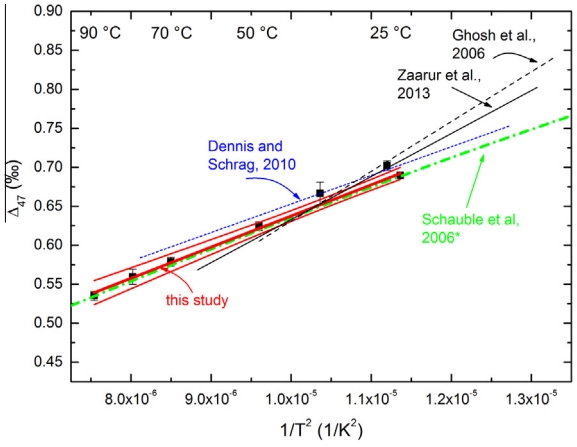

Fig. 5. Absolute Δ_{47} values of inorganic laboratory precipitates (filled squares) with linear regression (thick continuous line) and 95% confidence intervals (thin line above and below). Each data point represents the average of all measurements at this temperature including carbonates formed under NaCl-saturated conditions. Theoretical (dash-dotted line: Schauble et al., 2006; *with an acid fractionation correction after Passey and Henkes, 2012) and experimental calibrations (dashed line: Ghosh et al., 2006; short dashed line: Dennis et al., 2011; thin line: Zaarur et al., 2013) are given for comparison.

4. DISCUSSION

The addition of salt ions led to the precipitation of various $CaCO_3$ polymorphs and hydromagnesite which complicates a direct comparison of the results. Three different effects could influence the Δ_{47} value: ionic effects related to high salt concentrations, fractionation during phosphoric acid digestion depending on the specific mineral (Guo et al., 2009), and differences in the preferential formation of ^{13}C–^{18}O bonds for specific minerals during carbonate growth (Schauble et al., 2006). Current studies suggest that the Δ_{47} fractionation for different $CaCO_3$ polymorphs during phosphoric acid reaction is within analytical precision (Wacker et al., 2013; Defliese et al., 2015; see also Section 4.3). The Δ_{47} fractionation related to the acid digestion should be a constant value for a given mineralogy and digestion temperature, whereas a potential ionic effect is likely proportional to the ionic concentration, providing an opportunity to distinguish between both effects.

4.1. Effect of salt ions on ^{13}C–^{18}O clumping

We investigated the effect of salt ions on ^{13}C–^{18}O clumping relative to ions that are common in subsurface fluids, but also in seawater (Mg^{2+}, Ca^{2+}, Na^+, Cl^-). Samples related to NaCl addition (average concentration of 5.0 ± 0.9 molal) consist of several $CaCO_3$ polymorphs with the mineral structure depending whether the minerals formed in a NaCl-containing solution (mostly vaterite) or a NaCl-free fluid (calcite or aragonite). No significant differences were observed for experiments where the same $CaCO_3$ polymorphs were precipitated in both cases. For example, at 80 °C a calcite-dominated calcite–aragonite mixture was formed in the NaCl-free and the NaCl-saturated solution (there with a small vaterite contribution). Δ_{47} values of both laboratory precipitates are within 0.008 ± 0.021‰ of each other. Similarly, calcite and a calcite–aragonite mixture were precipitated at 25 °C in both experimental settings, yielding almost identical Δ_{47} values (difference: 0.008 ± 0.013‰). Both cases suggest that NaCl has no significant influence on ^{13}C–^{18}O clumping. At other experimental temperatures different $CaCO_3$ polymorphs were precipitated in both settings. Assuming mineral-specific effects to be negligible for $CaCO_3$ polymorphs (see Defliese et al., 2015) and comparing all samples from NaCl-free solutions with NaCl-saturated precipitates suggests no significant effect of the NaCl addition on the Δ_{47} value in the temperature range from 23 to 91 °C. The average deviation of $CaCO_3$ sample pairs from NaCl-free solutions and NaCl brine measured on the same machine

and at the same day is $-0.003 \pm 0.008‰$ (1σ; Fig. 2). Considering all samples from both machines similarly yields a negligible deviation between both sample sets of $-0.001 \pm 0.010‰$ (1σ). Note, that the effect of high NaCl concentrations and a potential mineral-specific effect (during growth or acid fractionation) could theoretically cancel each other in case of mixed $CaCO_3$ polymorphs. Therefore, our results strictly indicate only that the combined effect of NaCl addition and $CaCO_3$ polymorphism is negligible. We note, however, that these effects would have had to compensate for each other in several of our samples that contain various multiphase mixtures and were precipitated at a range of temperatures. We therefore deem this to be unlikely.

In contrast, the addition of $CaCl_2$ at 80 °C resulted in Δ_{47} offsets, in particular at elevated $CaCl_2$ concentration (Fig. 3). To substantiate these finding we repeated the precipitation at 25 °C and added in two independent experiments 50 and 100 g of $CaCl_2$, respectively. The first minerals at 25 °C were observed after 1 day ruling out rapid mineral formation as cause for the observed effects. Δ_{47} values at 25 °C are $0.713 \pm 0.016‰$ and $0.750 \pm 0.003‰$, higher than the $CaCl_2$-free reference value ($0.702 \pm 0.006‰$) and, thus, confirm the robustness of the trend of increasing offsets with increasing $CaCl_2$ concentration determined at the earlier precipitation experiments at 80°. Combining both experiments at 25 °C and 80 °C suggests an increase of the Δ_{47} values of +0.03 (± 0.01)‰ per mol $CaCl_2$ added to 1 liter solution ($R^2 = 0.72$; Fig. 3). Potential explanations for this offset are discussed in Section 4.2.

$MgCl_2(H_2O)_6$ addition resulted in the formation of hydromagnesite ($Mg_5(CO_3)_4(OH)_2{\cdot}4H_2O$) and brucite ($Mg(OH)_2$) with a minor, unidentifiable carbonate fraction. Experiments with a $MgCl_2(H_2O)_6$ concentration $\geqslant 2$ molal did not yield carbonate minerals within several weeks and were abandoned. The results of the hydromagnesite analyses are not directly comparable to the $CaCO_3$ minerals precipitated in the other experiments due to a potentially different acid fractionation factor. Differences of the measured Δ_{47} value relative to Mg-free samples could relate to the mineral structure (during growth and/or during acid digestion) or the Mg concentration of the solution. Lacking both theoretical and experimental acid fractionation factors for hydromagnesite and other hydrous carbonates we tentatively assume their acid digestion correction factor to be similar to $CaCO_3$ for a given acid reaction temperature. Based on this assumption, Δ_{47} values of hydromagnesite deviate negligibly from Mg-free minerals ($0.008 \pm 0.011‰$ and $0.011 \pm 0.015‰$; Fig. 4).

4.2. Interpretation of observed ionic effects

In the discussion of potential ionic effects we focus first on oxygen isotopes. The experiments of Taube (1954), Sofer and Gat (1972), and O'Neil and Truesdell (1991) sampled the unhydrated water that exchanges relative freely with the measured CO_2 collected above the water interface in their setup (i.e., in equilibrium with the free water). They found the free unhydrated water to be depleted in ^{18}O for structure-making electrolytes with a postulated enrichment of ^{18}O in the hydration spheres. In our experiments we observed the isotopic values related to the DIC via the precipitated carbonate. Insights into the oxygen isotope fractionation between hydrated and free water is mostly related to the unhydrated water with which the DIC freely exchanges. The exchange of oxygen isotopes in the hydration sphere of Ca or Mg with DIC during mineral formation is likely small as the time scales for oxygen isotope equilibration in the carbonate system are typically larger and on the order of minutes to hours at pH 8 and 25–40 °C (Zeebe and Wolf-Gladrow, 2001; Beck et al., 2005). An exception is hydromagnesite ($Mg_5(CO_3)_4(OH)_2{\cdot}4(H_2O)$) as part of the bound water in the hydration sphere may be included in the mineral structure.

An important parameter for ionic effects and their explanation is the dynamic hydration number which strongly varies for each ion and defines which portion of the total water fraction is bound in the hydration sphere. Na^+ and Cl^- have respectively a low (0.22) and negligible (0) dynamic hydration number (Kiriukhin and Collins, 2002), thus, have no tightly bound water molecules in their hydration spheres and are therefore expected to exert no influence on the isotopic values. The experiments of Taube (1954) and O'Neil and Truesdell (1991) confirm this expectation and exhibit no isotopic effects at addition of NaCl. Similarly, we do not observe a significant difference in the $\delta^{18}O$ value between the NaCl-free solution ($-6.7 \pm 0.9‰$) and the NaCl-saturated brine ($-7.1 \pm 0.9‰$). Mg^{2+} and Ca^{2+} have significantly higher dynamic hydration numbers (5.9 and 2.1, respectively; Kiriukhin and Collins, 2002) and, thus, lead to isotopic fractionation between free and hydrated water. The evolution of the $\delta^{18}O$ values with the ion concentration is illustrated in Fig.6 for free and hydrated water. The $\delta^{18}O$ values in the hydration sphere were calculated by using the pure water as reference and assuming partitioning of oxygen isotopes between hydration sphere and unhydrated water in dependence of the ion concentration and the dynamic hydration number. For both experiments with Mg and Ca addition more positive back-calculated solution $\delta^{18}O$ values relative to the unhydrated water are visible (Fig. 6). An exception is experiment Mg-1 which is consistent with the unhydrated water. In case of Ca^{2+} addition to the solution, more negative back-calculated solution $\delta^{18}O$ values would be expected as the hydration sphere is completely stripped off during mineral formation. However, high $CaCl_2$ concentrations are correlated with more positive back-calculated solution $\delta^{18}O$ values (Fig. 6). The consistently more positive back-calculated solution $\delta^{18}O$ values would contradict the observation of O'Neil and Truesdell (1991) if the carbonate mainly reflected unhydrated water. Non-equilibrium effects in general appear unlikely (such as due to rapid growth, insufficient isotopic equilibration of solution and DIC, or changes in the DIC composition due to increased salinity; see Supplementary). This holds in particular for the experiments at 25 °C where the temperature during preparation and equilibration of the solution and during carbonate precipitation was similar and close to room temperature. Salinity-driven changes in the DIC composition would

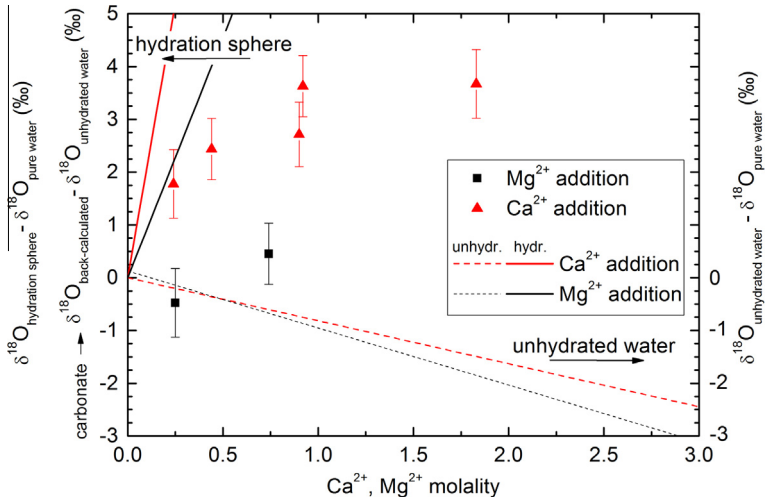

Fig. 6. Offset of the calculated water $\delta^{18}O$ values in Mg- (black squares) or Ca-bearing solutions (triangles) compared to the $\delta^{18}O$ value of unhydrated water that was prepared from reverse osmosis laboratory water (left axis). Results of CO_2 equilibration experiments using Mg- and Ca-containing solutions (calculated from O'Neil and Truesdell, 1991) are shown for comparison (dashed lines, right axis). Note the strong enrichment of ^{18}O in the hydration spheres (continuous lines) relative to the ^{18}O depletion in the unhydrated water (dashed lines).

cause more negative $\delta^{18}O$ values (Zeebe and Wolf-Gladrow, 2001) which are not observed. Rapid mineral formation could also be excluded (first minerals formed ~1 day after end of the equilibration phase) and, thus, in absence of other realistic causes the offset appears to be related to the presence of Ca^{2+} ions. Isotope exchange in a transition state related to the stripping off of water molecules from the hydration sphere and their preferential incorporation into the mineral could potentially explain elevated carbonate $\delta^{18}O$ values. Using the $\delta^{18}O$ values of the hydration sphere and the unhydrated water as end-members, the back-calculated solution water $\delta^{18}O$ yields a ~20% contribution from the hydration sphere. Stripping off hydrated water requires energy (e.g., Smith, 1977) and suggests that it is unlikely an instantaneous process and therefore provides some time for isotope exchange between water molecules from the hydration sphere and carbonate ions during mineral formation.

Hydromagnesite $\delta^{18}O$ values indicate solution $\delta^{18}O$ values that increase with electrolyte molality (Fig. 6). Hydromagnesite and back-calculated solution $\delta^{18}O$ values follow a trend with molality comparable in magnitude, but opposite in sign to that observed by O'Neil and Truesdell (1991) for the free unhydrated water. This indicates that a portion of hydrated water is included in hydromagnesite or influenced the DIC during the stripping off of the hydrated water. Note that we used the oxygen isotope fractionation factor $\alpha^{18}_{\text{carbonate-free water}}$ of salt-free water also for the brine due to the lack of a corresponding fractionation factor for brines.

In contrast to the oxygen isotope values that were calculated from the solution via the isotopic value of the carbonate and that were altered by isotope partitioning between hydration water and 'free' water, the occurrence of ^{13}C–^{18}O bonds in the carbonate mineral should be unaffected by hydration effects after isotopic equilibrium between hydrated and free water was reached. Under kinetic conditions, however, e.g., during fast mineral growth where attached water molecules are rapidly stripped off the hydration spheres, a discrimination may occur for ^{18}O in the water molecules between hydration water and 'free' water that finally affects the distribution of ^{12}C–^{16}O–^{16}O–^{16}O and ^{13}C–^{18}O–^{16}O–^{16}O. Analogous to oxygen isotopes we expect no influence on Δ_{47} from various NaCl concentrations, which is confirmed by our measurements (Fig. 2).

As we have no pure $CaCO_3$ in the Mg-related experiments (Table 1) a direct comparison with Mg-free minerals is difficult. Mg-addition caused the formation of hydromagnesite that exhibits a distinct structure and was expected to have a Δ_{47} acid fractionation factor different from calcite or aragonite (for magnesite: Schauble et al., 2006; Guo et al., 2009). Thus, a potential salt-ion effect during mineral formation may be super-imposed by effects during acid digestion of the carbonate. A cancelation of both effects is however unlikely and would only shift absolute values. A trend in the Δ_{47} values versus Mg^{2+} molality should be visible despite this complication. Hydromagnesite formed in this study at Mg concentrations of up to 0.4 molal and yielded no effect of Mg^{2+} on the Δ_{47} value (Fig. 4). This is consistent with expectations for clumped isotope equilibrium conditions. Hydromagnesite that grew at elevated Mg^{2+} concentrations contains four water molecules within its structure. Thus, there is the potential to accommodate the majority of the water molecules present in the hydration sphere of Mg^{2+} (5.9; Kiriukhin and Collins, 2002) directly into the mineral. This limits or prevents isotope exchange reactions in transition states, such as the stripping off of the water molecules from the Mg^{2+} ion, and provides a potential explanation for the missing effect of Mg concentration on the Δ_{47} value. The $\delta^{18}O$ value nevertheless increases as the water molecules in the hydration sphere are enriched in ^{18}O and incorporated indiscriminately in the mineral structure.

High $CaCl_2$ concentrations are correlated with Δ_{47} offsets that increase with the $CaCl_2$ concentration (Fig. 3).

This could have several causes which at least can be discarded for the 25 °C experiments (see Supplementary). The lack of temperature variations exclude effects related to the isotope equilibration time. Salt-addition increases the fraction of CO_3^{2-} within the DIC causing lower Δ_{47} values under fast growth conditions (Hill et al., 2014) which are not observed in our study. Instead, the correlation of Δ_{47} values with Ca^{2+} concentrations could be explained as a direct effect of the structure-making properties of Ca^{2+} ions in the solution and the isotopically different hydration sphere. Incomplete isotope exchange between carbonate ions and the ^{18}O-enriched hydration sphere of Ca^{2+} in a transition state during mineral formation (as also indicated by the $\delta^{18}O$ values) could also influence the abundance of the ^{13}C–^{18}O bonds and may explain the Δ_{47} offset from equilibrium. Therefore, the deviations from the expected Δ_{47} value are potentially caused by the presence and concentration of the Ca^{2+} ion.

Although our data set is limited it suggests that the salt ion effect on Δ_{47} values is small or negligible for NaCl. The small effect of $CaCl_2$ addition on Δ_{47} values and the missing effect for Mg addition provide a first insight into the role of hydration spheres and its isotopic influence during mineral formation. It also stresses the importance of a clear understanding of the mechanisms leading to the precipitation of Mg-bearing minerals to assess for potential salt-ion effects on the ^{13}C–^{18}O clumping.

4.3. Effect of mineral structure on ^{13}C–^{18}O clumping

Theoretical considerations suggest significant differences of the Δ_{47} value between various carbonate minerals and $CaCO_3$ polymorphs (Schauble et al., 2006; Guo et al., 2009). For example, aragonite and calcite that is precipitated at the same temperature is expected to differ by 0.02‰ at a 25 °C mineral formation temperature, with aragonite Δ_{47} values being higher than calcite Δ_{47} values.

Our laboratory precipitates provide an experimental data set for comparison with theoretical expectations. As the influence of salinity is negligible for NaCl (see Section 4.1) differences in the Δ_{47} value of the $CaCO_3$ polymorphs are either related to the phosphoric acid digestion or the ^{13}C–^{18}O clumping during mineral formation.

A linear regression of Δ_{47} over $1/T^2$ of aragonite/calcite mixtures and calcite reveals that both polymorphs of $CaCO_3$ yield similar results (Fig. 7). The linear fits are not statistically different from each other as the 95% confidence interval of both lines overlap (Fig. 7). A linear fit of the vaterite data agrees with the calcite results and the calcite/aragonite mixture line. Since we do not have pure aragonite samples, the aragonite/calcite mixture was taken as approximation for the aragonite Δ_{47}-T line. Therefore, the potential difference between aragonite and calcite may be underestimated, but still gives insight into the direction of change related to the mineral structure.

Given the similarity of the linear fits to the three $CaCO_3$ polymorphs, the effect of the $CaCO_3$ mineral structure on the ^{13}C–^{18}O clumping or the fractionation during acid digestion is at least limited (to <0.02‰ based on our data set) or at best negligible. A small difference between the

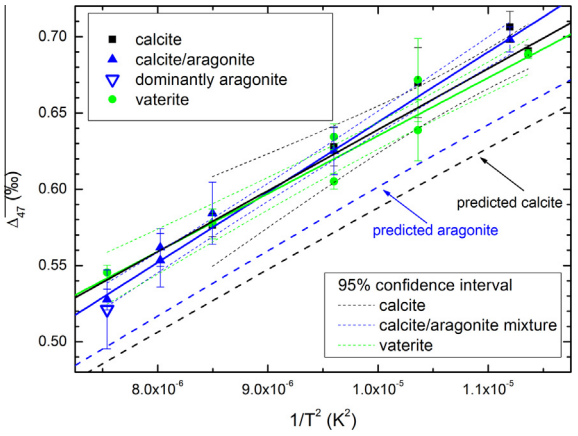

Fig. 7. Δ_{47} values of $CaCO_3$ polymorphs precipitated between 23 and 91 °C. At some temperatures (37, 50, 70, 91 °C) the precipitation experiment was repeated and resulted at 50, 70 and 91 °C in a different polymorph or mixture of $CaCO_3$ minerals. Linear error-weighted regressions including confidence intervals were done separately for different polymorphism (black line: calcite, green line: vaterite, blue line: aragonite-calcite). Theoretical predictions (Guo et al., 2009; dashed lines) are given for comparison. (For interpretation of the references to colour in this figure legend, the reader is referred to the web version of this article.)

Δ_{47} values of calcite and aragonite was observed in other studies (Eagle et al., 2013; Henkes et al., 2013; Wacker et al., 2013; Defliese et al., 2015), but the individual data sets do not support a significant difference between aragonite and calcite. The combined data suggest an effect close to the limit of current precision. For polymorphs being precipitated at the same temperature the work of Eagle et al.

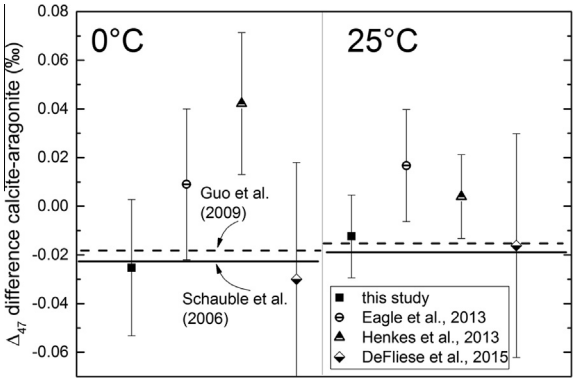

Fig. 8. Differences between the Δ_{47} values of pure calcite relative to aragonite crystals (or aragonite/calcite mixtures) of various experimental studies at two mineral formation temperatures. Both polymorphs were precipitated at the same temperature. Beyond this study values were taken from regression of data from Eagle et al. (2013), Henkes et al. (2013) and Defliese et al. (2015). The uncertainties were estimated based on the 95% confidence interval of the linear regression lines. For comparison, theoretical calculations of Schauble et al. (2006, thick line) and Guo et al. (2009, dashed line) are given. Note that the analytical precision of replicate sample measurements is typically on the order of ~0.015‰ (1 standard error).

(2013) and Henkes et al. (2013) yielded aragonite Δ_{47} values below those of calcite whereas our study and that of Defliese et al. (2015) yielded Δ_{47} values above those of calcite (Fig. 8). Summarizing all studies and comparing aragonite (or aragonite/calcite mixtures) with pure calcite at various temperatures (0 and 25 °C) yields slightly, but insignificantly lower Δ_{47} values for calcite (on average -0.002 ± 0.024‰). The agreement between calcite and aragonite opposes theoretical considerations that predict aragonite Δ_{47} values to be higher than calcite Δ_{47} values (Schauble et al., 2006; Guo et al., 2009). Note however, that in contrast to biogenic carbonates synthetic $CaCO_3$ polymorphs of Defliese et al. (2015) and our study agree within uncertainty with theoretical predictions.

Similar to the averaged results of the $CaCO_3$ polymorphs aragonite and calcite, no difference was observed in the Δ_{47} values of various other carbonates that were precipitated at the same temperature. Despite different mineral structure and chemical composition, carbonates in bioapatite and the carbonate siderite ($FeCO_3$) show Δ_{47} acid fractionation factors similar or identical to calcite (Eagle et al., 2010; Fernandez et al., 2014). This may suggests that the Δ_{47} value is largely determined in the DIC, i.e. in the bicarbonate and CO_3^{2-} at the typical pH range (~8), independent of the carbonate mineral structure.

5. CONCLUSIONS

Addition of different ions led to mineralogical variations in the precipitated carbonate, ranging from calcite and aragonite in pure $CaCO_3$ solutions to vaterite under NaCl-saturated conditions and hydromagnesite in Mg-containing water. $CaCl_2$ addition resulted in the formation of pure calcite. Therefore, the measured Δ_{47} value could be influenced simultaneously by ionic effects and mineral-specific fractionation during phosphoric acid digestion. However, ionic effects are expected to show a correlation with the ionic concentration, whereas the acid digestion fractionation should be a constant factor at a given temperature and carbonate mineralogy, providing a characteristic behaviour to disentangle both effects.

Clumped isotope values are identical for all carbonates precipitated at the same temperature, except for samples where $CaCl_2$ was added. This isotopic fractionation is potentially caused by a kinetic effect during stripping off water molecules from to the hydration sphere of the Ca^{2+} ion during carbonate growth. The good agreement between Δ_{47} values of carbonates with and without salt addition indicates a negligible influence of salt ions on ^{13}C–^{18}O clumping at least for NaCl and moderate Mg concentrations. Thus, $CaCO_3$ minerals (and hydromagnesite) precipitated in the ocean or from diagenetic-like fluids should follow the same Δ_{47}-T calibration for the investigated ions and ion concentrations. One potential exception to this rule is related to fluids with high Ca^{2+} concentrations, where the observed Δ_{47} offset of +0.03‰ per mole $CaCl_2$ in 1 l solution would translate into a maximum underestimation of the carbonate precipitation temperature by 10 °C at 25 °C, 20 °C at 100 °C, and 40 °C at 200 °C. It remains to be seen, however, whether this effect is present in natural brines that have a more complex chemistry involving a mixture of various ions.

No statistically significant effect of $CaCO_3$ polymorphism can be inferred as calcite, aragonite and vaterite share similar Δ_{47}-T relationships. Biogenic carbonates, that are either aragonitic, calcitic or a mixture of both, should be treated carefully with regard to the interpretation of the measured Δ_{47} values as the existence of a small offset between aragonite and calcite of <0.02‰ cannot be excluded based on the current empirical data set.

ACKNOWLEDGEMENT

We gratefully acknowledge funding from the Qatar Carbonates and Carbon Storage Research Centre (QCCSRC), provided jointly by Qatar Petroleum, Shell, and Qatar Science and Technology Park. We thank Annabel Dale, Anne-Lise Jourdan, and Simon Davis for support in mass spectrometer operation and in the calibration efforts, and the Carbonate Research group at Imperial College for fruitful discussions. We thank Jens Najorka for technical assistance during XRD measurements at the National History Museum London. We are grateful for thoughtful comments of anonymous reviewers and the associate editor R.H. Byrne that helped to improve the manuscript and thank Annabel Dale for proof reading and language revision.

APPENDIX A. SUPPLEMENTARY DATA

Supplementary data associated with this article can be found, in the online version, at http://dx.doi.org/10.1016/j.gca.2015.03.031.

REFERENCES

Affek H. P. (2013) Clumped isotopic equilibrium and the rate of isotope exchange between CO_2 and water. *Am. J. Sci.* **313**, 309–325.

Affek H. P. and Eiler J. M. (2006) Abundance of mass 47 CO_2 in urban air, car exhaust and human breath. *Geochim. Cosmochim. Acta* **70**, 1–12.

Alonso-Zarza A. M. and Tanner L. H. (2010) *Carbonates in Continental Settings: Geochemistry, Diagenesis and Applications*. Elsevier, Amsterdam.

Beck W. C., Grossman E. L. and Morse J. W. (2005) Experimental studies of oxygen isotope fractionation in the carbonic acid system at 15°, 25° and 40 °C. *Geochim. Cosmochim. Acta* **69**, 3493–3503.

Blanton T. N., Huang T. C., Toraya H., Hubbard C. R., Robie S. B., Louër D., Göbel H. E., Will G., Gilles R. and Raftery T. (1995) JCPDS-International Centre for Diffraction Data round robin study of silver behenate. A possible low-angle X-ray diffraction calibration standard. *Powder Diffr.* **10**, 91–95.

Böhm F., Joachimski M. M., Dullo W. C., Eisenhauer A., Lehnert H., Reitner J. and Worheide G. (2000) Oxygen isotope fractionation in marine aragonite of coralline sponges. *Geochim. Cosmochim. Acta* **64**, 1695–1703.

Bristow T. F., Bonifacie M., Derkowski A., Eiler J. M. and Grotzinger J. P. (2011) A hydrothermal origin for isotopically anomalous cap dolostone cements from south China. *Nature* **474**, 68–72.

Budd D. A., Frost, III, E. L., Huntington K. W. and Allwardt P. F. (2013) Syndepositional deformation features in high-relief carbonate platforms: long-lived conduits for diagentic fluids. *J. Sediment. Res.* **82**, 12–36.

Came R. E., Eiler J. M., Veizer J., Azmy K., Brand U. and Weidman C. R. (2007) Coupling of surface temperatures and atmospheric CO_2 concentrations during the Palaeozoic era. *Nature* **449**, 198–202.

Came R. E., Brand U. and Affek H. P. (2014) Clumped isotope signatures in modern brachiopod carbonate. *Chem. Geol.* **377**, 20–30.

Cao X. and Liu Y. (2012) Theoretical estimation of the equilibrium distribution of clumped isotopes in nature. *Geochim. Cosmochim. Acta* **77**, 292–303.

Csank A. Z., Tripati A. K., Patterson W. P., Eagle R. A., Rybczynski N., Ballantyne A. P. and Eiler J. M. (2011) Estimates of Arctic land surface temperatures during the early Pliocene from two novel proxies. *Earth Planet. Sci. Lett.* **304**, 291–299.

Darling W. G., Bath A. H. and Talbot J. C. (2003) The O&H stable isotopic composition of fresh waters in the British Isles. 2. Surface waters and groundwater. *Hydrol. Earth Syst. Sci.* **7**, 183–195.

Das Sharma. S., Patil D. J. and Gopalan K. (2002) Temperature dependence of oxygen isotope fractionation of CO_2 from magnesite-phosphoric acid reaction. *Geochim. Cosmochim. Acta* **66**, 589–593.

Defliese W. F., Hren M. T. and Lohmann K. C. (2015) Compositional and temperature effects of phosphoric acid fractionation on Δ_{47} analysis and implications for discrepant calibrations. *Chem. Geol.* **396**, 51–60.

Dennis K. J. and Schrag D. P. (2010) Clumped isotope thermometry of carbonatites as an indicator of diagenetic alteration. *Geochim. Cosmochim. Acta* **74**, 4110–4122.

Dennis K. J., Affek H. P., Passey B. H., Schrag D. P. and Eiler J. W. (2011) Defining an absolute reference frame for 'clumped' isotope studies of CO_2. *Geochim. Cosmochim. Acta* **75**, 7117–7131.

Driesner T. and Seward T. M. (2000) Experimental and simulation study of salt effects and pressure/density effects on oxygen and hydrogen stable isotope liquid-vapor fractionation for 4–5 molal aqueous NaCl and KCl solutions to 400 °C. *Geochim. Cosmochim. Acta* **64**, 1773–1784.

Eagle R. A., Schauble E. A., Tripati A. K., Tütken T., Hulbert R. C. and Eiler J. M. (2010) Body temperatures of modern and extinct vertebrates from ^{13}C to ^{18}O bond abundances in bioapatite. *PNAS* **107**, 10377–10382.

Eagle R. A., Tütken T., Martin T. S., Tripati A. K., Fricke H. C., Connely M., Cifelli R. L. and Eiler J. M. (2011) Dinosaur body temperatures determined from isotopic (^{13}C–^{18}O) ordering in fossil biominerals. *Science* **333**, 443–445.

Eagle R. A., Eiler J. M., Tripati A. K., Ries J. B., Freitas P. S., Hiebenthal C., Wanamaker, Jr, A. D., Taviani M., Elliot M., Marenssi S., Nakamura K., Ramirez P. and Roy K. (2013) The influence of temperature and seawater carbonate saturation state on ^{13}C–^{18}O bond ordering in bivalve mollusks. *Biogeosciences* **10**, 4591–4606.

Eiler J. M. (2007) "Clumped-isotope" geochemistry- The study of naturally-occurring, multiply-substituted isotopologues. *Earth Planet. Sci. Lett.* **262**, 309–327.

Eiler J. M. and Schauble E. (2004) $^{18}O^{13}C^{16}O$ in Earth's atmosphere. *Geochim. Cosmochim. Acta* **68**, 4767–4777.

Emiliani C. (1955) Pleistocene temperatures. *J. Geol.* **63**, 538–578.

Fernandez A., Tang J. and Rosenheim B. (2014) Siderite 'clumped' isotope thermometer: a new paleoclimate proxy for humid continental environments. *Geochim. Cosmochim. Acta* **126**, 411–421.

Frank H. S. and Wen W.-Y. (1957) Ion-solvent interaction, structural aspects of ion-solvent interaction in aqueous solutions: a suggested picture of water structure. *Discuss. Faraday Soc.* **24**, 133–140.

Friedman I. and O'Neil J. R. (1977) Compilation of stable isotope fractionation factors of geochemical interest. U.S. Geological Survey Professional paper No. 440-KK, 1–12.

Ghosh P., Adkins J., Affek H. P., Balta B., Guo W., Schauble E. A., Schrag D. and Eiler J. M. (2006) ^{13}C–^{18}O bonds in carbonate minerals: a new kind of paleothermometer. *Geochim. Cosmochim. Acta* **70**, 1439–1456.

Grauel A.-L., Schmid T. W., Hu B., Bergami C., Capotondi L., Zhou L. and Bernasconi S. M. (2013) Calibration and application of the 'clumped isotope' thermometer to foraminifera for high-resolution climate reconstructions. *Geochim. Cosmochim. Acta* **108**, 125–140.

Guo W., Mosenfelder J. L., Goddard, III, W. A. and Eiler J. M. (2009) Isotopic fractionations associated with phosphoric acid digestion of carbonate minerals: Insights from first-principles theoretical modeling and clumped isotope measurements. *Geochim. Cosmochim. Acta* **73**, 7203–7225.

Halevy I., Fischer W. W. and Eiler J. M. (2011) Carbonates in the martian meteorite Allan Hills 84001 formed at 18 ± 4°C in a near-surface aqueous environment. *PNAS* **108**, 16895–16899.

Hanor J. S. (1994) Origin of saline fluids in sedimentary basins. In *Geofluids: Origin, migration and evolution of fluids in sedimentary basins* (ed. J. Parnell). Geological Society, London, pp. 151–174, Special Publications No.78.

Henkes G. A., Passey B. H., Wanamaker, Jr, A. D., Grossman E. L., Ambrose, Jr, W. G. and Carrol M. L. (2013) Carbonate clumped isotope compositions of modern marine mollusk and brachiopod shells. *Geochim. Cosmochim. Acta* **106**, 307–325.

Hill P. S., Tripati A. K. and Schauble E. A. (2014) Theoretical constraints on the effects of pH, salinity, and temperature on clumped isotope signatures of dissolved inorganic carbon species and precipitating carbonate minerals. *Geochim. Cosmochim. Acta* **125**, 610–652.

Hren M. T., Sheldon N. D., Grimes S. T., Collinson M. E., Hooker J. J., Bugler M. and Lohmann K. C. (2013) Terrestrial cooling the northern Europe during the Eocene-Oligocene transition. *PNAS* **110**, 7562–7567.

Huntington K. W., Eiler J. M., Affek H. P., Guo W., Bonifacie M., Yeung L. Y., Thiagarajan N., Passey B., Tripati A., Daëron M. and Came R. (2009) Methods and limitations of 'clumped' CO_2 isotope (Δ_{47}) analysis by gas-source isotope ratio mass spectrometry. *J. Mass Spectrom.* **44**, 1318–1329.

Huntington K. W., Budd D. A., Wernicke B. P. and Eiler J. M. (2011) Use of clumped-isotope thermometry to constrain the crystallization temperature of diagenetic calcite. *J. Sediment. Res.* **81**, 656–669.

Keating-Bitonti C. R., Ivany L. C., Affek H. P., Douglas P. and Samson S. D. (2011) Warm, not super-hot, temperatures in the early Eocene subtropics. *Geology* **39**, 771–774.

Kim S. T. and O'Neil J. R. (1997) Equilibrium and nonequilibrium oxygen isotope effects in synthetic carbonates. *Geochim. Cosmochim. Acta* **61**, 3461–3475.

Kim S.-T., O'Neil J. R., Hillaire-Marcel C. and Mucci A. (2007a) Oxygen isotope fractionation between synthetic aragonite and water: influence of temperature and Mg^{2+} concentration. *Geochim. Cosmochim. Acta* **71**, 4704–4715.

Kim S.-T., Mucci A. and Taylor B. E. (2007b) Phosphoric acid fractionation factors for calcite and aragonite between 25 and 75 °C: revisited. *Chem. Geol.* **246**, 135–146.

Kim S.-T., Park S.-S. and Yun S.-T. (2012) Influence of dissolved ions on determination of oxygen isotope composition of aqueous solutions using the CO_2–H_2O equilibration method. *Rapid Commun. Mass. Spectrom.* **26**, 2083–2092.

Kiriukhin M. Y. and Collins K. D. (2002) Dynamic hydration numbers for biologically important ions. *Biophys. Chem.* **99**, 155–168.

Kluge T. and John C. M. (2014) Technical note: a simple method for vaterite precipitation in isotopic equilibrium: implications for bulk and clumped isotope analysis. *Biogeosci. Discuss.* **11**, 17361–17390.

Kluge T., John C. M., Jourdan A.-L., Davis S. and Crawshaw J. (2015) Laboratory calibration of the calcium carbonate clumped isotope thermometer in the 25–250°C temperature range. *Geochim. Cosmochim. Acta* **157**, 213–227.

McCrea J. M. (1950) On the isotopic chemistry of carbonates and a paleotemperature scale. *J. Chem. Phys.* **18**, 849–857.

Miliman J. D. (1974) *Marine Carbonates*. Springer, Berlin, Heidelberg, New York.

Moore C. H. (2001) *Carbonate Reservoirs. Developments in Sedimentology*. Elsevier, Amsterdam.

Newell K. D. and Goldstein R. H. (1999) A new technique for surface and shallow subsurface paleobarometry using fluid inclusions: an example from the Upper Ordovician Viola Formation, Kansas, USA. *Chem. Geol.* **154**, 97–111.

O'Neil J. R. and Barnes I. (1971) C^{13} and O^{18} compositions in some fresh-water carbonates associated with ultramafic rocks and serpentinites: western United States. *Geochim. Cosmochim. Ac.* **35**, 687–697.

O'Neil J. R., Clayton R. N. and Mayeda T. K. (1969) Oxygen isotope fractionation in divalent metal carbonates. *J. Chem. Phys.* **51**, 5547–5558.

O'Neil J. R. and Truesdell A. H. (1991) Oxygen isotope fractionation studies of solute-water interaction. In *Stable Isotope Geochemistry: A Tribute to Samuel Epstein* (eds. H. P. Taylor, J. R. O'Neil and I. R. Kaplan). The Geochemical Society, San Antonio, USA, Special Publication No.3.

Passey B. H. and Henkes G. A. (2012) Carbonate clumped isotope bond reordering and geospeedometry. *Earth Planet. Sci. Lett.* **351–352**, 223–236.

Passey B. H., Levin N. E., Cerling T. E., Brown F. H. and Amd Eiler J. M. (2010) High- temperature environments of human evolution in East Africa based on bond ordering in paleosol carbonates. *PNAS* **107**, 11245–11249.

Rossi C., Goldstein R. H., Ceriani A. and Marfil R. (2002) Fluid inclusions record thermal and fluid evolution in reservoir sandstones, Khatatba Formation, Western Desert, Egypt: A case for fluid injection. *AAPG Bull.* **86**, 1774–1799.

Saenger C., Affek H. P., Felis T., Thiagarajan N., Lough J. M. and Holcomb M. (2012) Carbonate clumped isotope variability in shallow water corals: temperature dependence and growth-related vital effects. *Geochim. Cosmochim. Acta* **99**, 224–242.

Schauble E. A., Ghosh P. and Eiler J. M. (2006) Preferential formation of ^{13}C–^{18}O bonds in carbonate minerals, estimated using first-principle lattice dynamics. *Geochim. Cosmochim. Acta* **70**, 2510–2529.

Shackleton, N.J., Opdyke, N.D., 1976. Oxygen isotope and paleomagnetic stratigraphy of Equatorial Pacific core V28–239, late Pliocene to latest Pleistocene. In: Cline, R.M., Hays, J.D. (Eds.), Investigation of Later Quaternary Paleoceanography and Paleoclimatology. Geol. Soc. Am. Mem., vol. 145, Geological Society of America, Boulder, pp. 449–464.

Smith D. W. (1977) Ionic hydration enthalpies. *J. Chem. Educ.* **54**, 540–542.

Sofer Z. and Gat J. R. (1972) Activities and concentrations of oxygen-18 in concentrated aqueous salt solutions: analytical and geophysical implications. *Earth Planet. Sci. Lett.* **15**, 232–238.

Tang J., Dietzel M., Fernandez A., Tripati A. K. and Rosenheim B. E. (2014) Evaluation of kinetic effects on clumped isotope fractionation (Δ_{47}) during inorganic calcite precipitation. *Geochim. Comsochim. Acta* **134**, 120–136.

Tarutani T., Clayton R. N. and Mayeda T. K. (1969) The effect of polymorphism and magnesium substitution on oxygen isotope fractionation between calcium carbonate and water. *Geochim. Cosmochim. Acta* **33**, 987–996.

Taube H. (1954) Use of oxygen isotope effects in the study of hydration of ions. *J. Chem. Phys.* **58**, 523–528.

Tripati A. K., Eagle R. A., Thiagarajan N., Gagnon A. C., Bauch H., Halloran P. R. and Eiler J. M. (2010) ^{13}C–^{18}O isotope signatures and 'clumped isotope' thermometry in foraminfera and coccoliths. *Geochim. Cosmochim. Acta* **74**, 5697–5717.

Tucker M. E. and Bathurst R. G. C. (1990) *Carbonate Diagensis*. Blackwell Scientific Publications, Oxford.

Uchikawa J. and Zeebe R. E. (2012) The effect of carbonic anhydrase on the kinetics and equilibrium of the oxygen isotope exchange in the CO_2-H_2O system: Implications for $\delta^{18}O$ vital effects in biogenic carbonates. *Geochim. Cosmochim. Acta* **95**, 15–34.

Wacker U., Fiebig J. and Schoene B. R. (2013) Clumped isotope analysis of carbonates: comparison of two different acid digestion techniques. *Rapid Commun. Mass Spectrom.* **27**, 1631–1642.

Wang Z., Schauble E. A. and Eiler J. M. (2004) Equilibrium thermodynamics of multiply substituted isotopologues of molecular gases. *Geochim. Cosmochim. Acta* **68**, 4779–4797.

Warren J. K. (2006) *Evaporites: Sediments, Resources and Hydrocarbons*. Springer, Berlin, Heidelberg.

Wilkinson J. J. (2001) Fluid inclusions in hydrothermal ore deposits. *Lithos* **55**, 229–272.

Zaarur S., Affek H. P. and Brandon M. (2013) A revised calibration of the clumped isotope thermometer. *Earth Planet. Sci. Lett.* **382**, 47–57.

Zachos J., Pagani M., Sloan L., Thomas E. and Billups K. (2001) Trends, rhythms, and aberrations in global climate 65 Ma to present. *Science* **292**, 686–693.

Zedef V., Russell M. J., Fallick A. E. and Hall A. J. (2000) Genesis of vein stockwork and sedimentary magnesite and hydromagnesite deposits in the ultramafic terranes of southwestern Turkey: a stable isotope study. *Econ. Geol.* **95**, 429–446.

Zeebe R. E. and Wolf-Gladrow D. (2001) *CO_2 in Seawater: Equilibrium, Kinetics, Isotopes*. Elsevier, Amsterdam.

Associate editor: Robert H. Byrne